Performance Improvement of Solar Steam Generation Systems Using the Plasmonic Effect of Titanium Nitride

PRAVIN ALIAKBARI [1], **FARZANEH ARABPOUR ROGHABADI** [1,*], **AND SEYED MOJTABA SADRAMELI** [2]

[1] *Department of Process Engineering, Tarbiat Modares University, Tehran, Iran*
[2] *Department of Engineering, German University of Technology in Muscat, Oman*
[*] *Corresponding author email: Arabpour@modares.ac.ir*

Manuscript received 14 December, 2021; revised 24 April, 2022; accepted 27 May, 2022. Paper no. JEMT-2112-1357.

Today, access to freshwater is one of the important human needs. Although the conventional methods for obtaining freshwater through recycling or desalination of water are very efficient; they consume high energy and are costly. Solar energy as a sustainable, accessible, and pollution-free energy can be a suitable source of energy to obtain freshwater. Solar steam generation through surface evaporation is a promising technology to achieve high-quality freshwater without the use of solar concentrators. These systems consist a floating substrate that is covered by photothermal material to harvest the sun energy. The water is transferred to the surface and evaporated by heat localization. In this study, two-layer systems consisting of polyurethane foam substrate and titanium nitride light absorber are fabricated and used for solar desalination. The studied system, in the best case, has an evaporation rate of 1.31 $kg/(m^2h^1)$ which is equivalent to an efficiency of 84%. According to the results, titanium nitride nanoparticles provide efficient light absorption due to owning plasmonic effect.

keywords: *Solar Desalination, Solar Steam Generation, Polyurethane Foam, Titanium Nitride, Light Absorber.*

http://dx.doi.org/10.22109/JEMT.2022.319405.1357

1. INTRODUCTION

Water is essential for environment and the growth of human society. Due to the increasing of the population of the world, the growing trend of urbanization, and climate change, half of the world's population is going to be affected by water stress by 2030 [1]. The amount of freshwater on the ground is constant though it needs to be treated for achieving freshwater. According to the World Health Organization (WHO), the permissible water salinity is 500 - 1000 ppm, while the salinity of seawater is 35000 - 45000 ppm [2].

The use of solar energy as a heating source in areas such as power generation, residential water heaters, desalination, and wastewater treatment has received a lot of attention [3]. Solar steam generation technologies are divided into direct and indirect methods. The direct method uses solar energy directly to desalinate water, while in the indirect one, the solar energy firstly is converted into another form of energy such as electrical and then is used for water desalination [4]. The production of water vapor at a temperature of 100 ° C under sunlight requires the use of optical concentrators but in addition to being expensive, this method also requires structural support [3], [5]. In the method without optical concentrators, solar energy is usually received by a solar absorber and then converted to heat [4]. Different configurations have been used for direct solar water steam generation (Figure1). As shown in Figure 1a, the absorber is located on the bottom of the container and is heated from the bottom. In this method, the energy losses are high and heat localization can not occurred efficiently. Because, the harvested energy is consumed to heat the bulk water and also some of the incident photons are reflected from the water surface, leading to a relatively low efficiency (30-55%) [6], [7].

In the nanofluid mode, light absorber nanoparticles are dispersed in water, providing better performance compared to the first configuration though it still suffers from the heat losses (Figure 1 a and b) [8]. Recently, floating solar steam generation systems have been used to generate steam in the air-water interface as shown in Figure 1c [9]. The goal of this method is to heat the water at the air-water interface, not the bulk water. This approach has shown high solar steam generation efficiency [10]. In general, generating steam efficiently by using floating structures requires the following three key factors:

- High ability to absorb sunlight.

Fig. 1. Schematic of (a) underfloor heating mode; (b) nanofluid mode (c) floating mode of solar steam generation

- Minimal heat loss to the bulk of water.
- Transfer water to the evaporation surface for continuous steam generation [11].

The use of black photothermal layers is a new strategy that harvests solar energy and converts it into heat [12]. Carbon nanotubes and graphene have high light absorption due to SP2 hybridization and π bond formation [13]. Metal nanoparticles, semiconductor nanostructures, carbon, and black polymer nanomaterials have been also used as light absorbers [14]. To achieve a high thermal efficiency for selected absorbers, they should have a high light absorption coefficient (α) and low emission (ϵ) [3]. Reducing convective, conductive, and radiative losses can significantly improve the energy efficiency of the system [15]. Researchers used carbon foam and wood as thermal insulation layers with thermal conductivity coefficients of 0.04 $W/(m^1k^1)$ and 0.17 $W/(m^1k^1)$ respectively, to prevent thermal losses [16], [17]. To supply water at the evaporation surface, it is necessary to design water transfer channels from the bulk to the surface. As reported, graphene oxide was used to transfer water to the surface through its porous column. The transfer occurs due to the capillary forces, leading an evaporation rate of 1.27 $kg/(m^2h^1)$ [18].

In this study, fabrication of the solar steam generation system is focused which is environmentally friendly and economically viable. In order to reduce the heat losses which are considered as the major challenges of solar steam generation systems, polyurethane (PU) with low thermal conductivity is used. Also, felt is utilized as a water transporter because of its high hydrophilicity and high ability to transfer water from the bulk water to the system surface. Titanium nitride (TiN) is used as the absorber layer due to its high plasmonic effect. Systems containing different amounts of TiN are fabricated and analyzed to achieve the optimum level of the TiN nanoparticles.

2. METHODOLOGY

To produce PU foam, the resin (ISO 370) and its curing agent (Polymoc 327/B2) are mixed with the ratio of 1:1 and subsequently moved to the Teflon cylindrical mold. The mixture is then stirred by a mechanical stirrer for 20 seconds and kept under ambient temperature and pressure for shaping the foam. The physical properties of PU foam precursors are presented in Table (1).

To prepare the absorber layer, different amounts of TiN are mixed with 3500 mg of deionized water and 200 mg of acrylic resin in an ultrasonic for 10 minutes. Then the felt is cut into a circle with a diameter of 5 cm and all of the prepared absorber mixture is deposited on the felt with a brush. To study the effect of the TiN concentration on the performance, systems containing 0.047 wt%, 0.11 wt%, 0.2 wt%, 0.27 wt%, 0.33 wt%, and 0.5 wt%

Table 1. Physical characteristics of PU foam precursors.

Materials	Specific weight (gr/m^3)	Viscosity(m.Pa.s)
resin (ISO 370)	1.23	180-270
curing agent (Polymoc 327/B2)	1.1	1200-1600

of TiN are fabricated and analyzed. Weight percentage of TiN is calculated by dividing the amount of titanium nitride to the sum of titanium nitride and 200 mg of acrylic resin. The absorber layer is then dried in an oven at 120 ° C for 15 minutes. To calculate the efficiency of solar steam generation system, equation (1) is used, where Qs represents the equivalent solar power ($1KW/m^2$) and Qe represents the amount of power required to evaporate water calculated by equation (2).

$$\eta = \frac{Q_e}{Q_s} \tag{1}$$

$$Q_e = H_v \times \frac{dm}{dt} = H_e \times r \tag{2}$$

H_v is the enthalpy of water evaporation, which is approximately equal to $2260Kj/Kg$. Moreover, m is the amount of water evaporated, t is the time, and r is the water evaporation rate (WER) obtained from the linear fit of the graph of mass changes in time.

A. Characterization

The microstructure study of the absorber layer is performed using FESEM (MIRA3TESCAN-XMU). Leica light microscope is used to observe the absorber surface. The hydrophilicity and hydrophobicity of the absorber layers are investigated using the contact angle device (Jikan-CAG20).

The thermal test is performed using a model thermographic camera (OLIP ThermoCam P200). To perform this test, the built-in solar systems are placed under the light of a sun simulator and then an imaging is performed using the thermographic camera.

3. RESULTS

In Fig.2a, the SEM images of TiN nanoparticles are presented. As observed the nanoparticles have coral-like structures and the average dimension of nanoparticles is 38 nm.

Fig 2b shows the XRD pattern of TiN nanoparticles. Five strong diffraction peaks are observed at 2θ equals to 44 °, 50 °, 74 °, 89 °, 94 °, corresponding to plates (111), (002), (022), (113) and (222) in the structure, respectively. It indicates the high crystallinity and purity of TiN. The crystal structure of TiN nanoparticles is a centered cube with a lattice parameter of 4.24 Å.

Fig 2c shows the visible-ultraviolet absorption spectrum of TiN nanoparticles at wavelengths of 200 to 850 nm. The 583 nm peak relates to the plasmonic effect [19] due to the interband interactions of free electrons that can support local surface plasmonic resonance [20]–[22].

To study the morphology of the absorber layer, FESEM images are prepared from the absorber layer. In the solar steam production system, felt is used as a water transporter and a substrate for absorber materials. Fig. 3a and b depict the FESEM images of the pure felt and TiN absorber layer. It contains felt with TiN 0.27 wt% and acrylic adhesive. As shown in the fig. 3b,

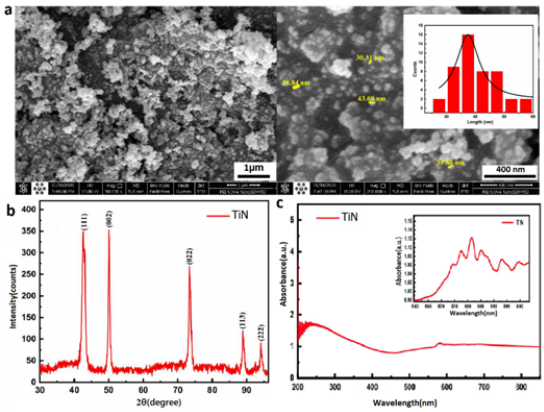

Fig. 2. (a) SEM image of TiN nanoparticles; (b) XRD patterns of TiN nanoparticles; (c) UV-vis-NIR absorption spectra of TiN nanoparticles.

the absorbers are uniformly dispersed on the surface of the felt filaments and some of the pores of the felt.

Fig. 3c is an optical microscope image of the absorber surface of TiN. The contact angle of the surface of TiN absorber is 74 degrees, confirming the hydrophilicity of the surface.

The WER in the presence of TiN increases significantly compared to PU foam and uncovered water due to the high light absorption. Among the different samples, the highest WER and solar steam conversion efficiency is achieved when the absorber amount of TiN 0.27 wt% of TiN is used. When the amount of TiN absorber is less than TiN 0.27 wt%, the WER and the efficiency show ascending trend. However, when the amount of TiN absorber is more than 0.27 wt%, the WER and solar vapor conversion efficiency decrease with the increase of the TiN. It seems that in the presence of high amount of TiN, some of the pores available in felt are blocked. As a result, water transfer process faces problem, leading the reduction of the performance. Moreover, heat losses from the surface through TiN emission can also be another reason for this performance reduction.

As shown in Table 2, the WER for uncovered water under one-sun is 0.45 $kg/(m^2h^1)$. This value is 0.71 $kg/(m^2h^1)$ for a PU+felt system floating on water. By adding TiN 0.27 wt% on PU insulation (a two-layer system), the WER of 1.34 $kg/(m^2h^1)$ is achieved which is more than twice the value of uncovered water.

Fig. 4a shows the water mass change of the solar steam generation systems. The water mass change for uncovered water was 0.45 kg/m^2 and for PU and TiN75 were 0.71 kg/m^2, 1.34 kg/m^2, respectively. Fig. 4b shows the efficiency of the solar steam generation systems. As can be seen, the efficiency of steam generation for uncovered water is 28%. With the presence of floating PU insulating layer and absorber layer, the efficiency increases to 84%. The results show that TiN can efficiently harvest the sun light since it has plasmonic effect.

The thermal profile of the samples is shown in Fig. 4c. As seen, when tap water covered by only PU insulating layer is placed under the solar simulator, the heat is distributed throughout the bulk water and there is no significant difference between the surface temperature and the bulk temperature. While, with the addition of the absorber layer on the PU insulating layer, the temperature difference between the surface and the bulk water reaches its maximum. As a result, TiN absorber layer absorbs the incident light efficiently and the PU foam successfully localizes it.

In Fig. 4d, water temperature of surface at first is 27°C and after being under the solar simulator for 60 minutes reaches 34°C. In the presence of thermal insulation (single layer system or PU) it increases to 40°C and in the presence of thermal insulation and absorber layer (two-layer system or PU+ TiN 0.27 wt%) reaches 45°C. Temperature, steam generation rate, mass changes, and efficiency of TiN absorber based systems are summarized in Table (2).

Table 2. Temperature, steam generation rate, the efficiency of different systems.

Sample	Surface temperature after illumination (°C)	Temperature difference (°C)	Evaporation Rate (kg/m^2h)	Efficiency (%)
Pure water	34	7	0.45	28
PU	40	13	0.71	45
TiN0.047 wt%	42.1	15.1	1.19	75
TiN0.11 wt%	42.5	15.5	1.27	80
TiN0.2 wt%	42.8	15.8	1.29	81
TiN0.27 wt%	45	18	1.34	84
TiN0.33 wt%	43.5	16.5	1.30	82
TiN0.5 wt%	43.1	16.1	1.29	81

4. CONCLUSION

In summary, two-layer solar steam generation systems were fabricated and their performances were compared with the performance of uncovered water and PU foam insulator. In the two-layer system, TiN with different concentrations was used as the light absorber because of its plasmonic effects. Evaporated water rates for pure water and single-layer system and the best two-layer system were 0.45 $kg/(m^2h^1)$, 0.71$kg/(m^2h^1)$ and 1.34 $kg/(m^2h^1)$, respectively. The efficiency of steam generation for pure water was 28%, while it was 45% and 84% for PU foam and two-layer systems, respectively.

REFERENCES

[1] UNEP, "Options for Decoupling Economic Growth from Water use and Water Pollution," Options Decoupling Econ. Growth from Water use Water Pollut., 2016, doi: 10.18356/d38f0de2-en.

[2] G. N. Tiwari, H. N. Singh, and R. Tripathi, "Present status of solar distillation," Sol. Energy, vol. 75, no. 5, pp. 367–373, 2003, doi: 10.1016/j.solener.2003.07.005.

[3] G. Ni et al., "Steam generation under one sun enabled by a floating structure with thermal concentration," Nat. Energy, vol. 1, no. 9, pp. 1–7, 2016.

[4] Y. Li et al., "3D-Printed, All-in-One Evaporator for High-Efficiency Solar Steam Generation under 1 Sun Illumination," Adv. Mater., vol. 29, no. 26, pp. 1–8, 2017, doi: 10.1002/adma.201700981.

[5] W. Shang and T. Deng, "Solar steam generation: Steam by thermal concentration," Nat. Energy, vol. 1, no. 9, pp. 1–2, 2016, doi: 10.1038/nenergy.2016.133.

[6] A. E. Kabeel and S. A. El-Agouz, "Review of researches and developments on solar stills," Desalination, vol. 276, no. 1–3, pp. 1–12, 2011.

[7] P. Zhang, Q. Liao, H. Yao, Y. Huang, H. Cheng, and L. Qu, "Direct solar steam generation system for clean water production," Energy Storage Mater., vol. 18, pp. 429–446, 2019, doi: 10.1016/j.ensm.2018.10.006.

[8] T. P. Otanicar, P. E. Phelan, R. S. Prasher, G. Rosengarten, and R. A. Taylor, "Nanofluid-based direct absorption solar collector," J. Renew. Sustain. energy, vol. 2, no. 3, p. 33102, 2010.

[9] Z. Wang et al., "Bio-inspired evaporation through plasmonic film of nanoparticles at the air-water interface," Small, vol. 10, no. 16, pp. 3234–3239, 2014, doi: 10.1002/smll.201401071.

[10] Y. Shi et al., "A 3D Photothermal Structure toward Improved Energy Efficiency in Solar Steam Generation," Joule, vol. 2, no. 6, pp. 1171–1186, 2018, doi: 10.1016/j.joule.2018.03.013.

[11] Q. Zhang, W. Xu, and X. Wang, "Carbon nanocomposites with high photothermal conversion efficiency," Sci. China Mater., vol. 61, no. 7, pp. 905–914, 2018, doi: 10.1007/s40843-018-9250-x.

[12] G. Liu, J. Xu, and K. Wang, "Solar water evaporation by black photothermal sheets," Nano Energy, vol. 41, no. September, pp. 269–284, 2017, doi: 10.1016/j.nanoen.2017.09.005.

[13] Y. Zhao, Q. Han, Z. Cheng, L. Jiang, and L. Qu, "Integrated graphene systems by laser irradiation for advanced devices," Nano Today, vol. 12, pp. 14–30, 2017, doi: 10.1016/j.nantod.2016.12.010.

[14] G. Wang et al., "Reduced Graphene Oxide-Polyurethane Nanocomposite Foam as a Reusable Photoreceiver for Efficient Solar Steam Generation," Chem. Mater., vol. 29, no. 13, pp. 5629–5635, 2017, doi: 10.1021/acs.chemmater.7b01280.

[15] F. Zhao et al., "Highly efficient solar vapour generation via hierarchically nanostructured gels," Nat. Nanotechnol., vol. 13, no. 6, pp. 489–495, 2018, doi: 10.1038/s41565-018-0097-z.

[16] H. Ghasemi et al., "Solar steam generation by heat localization," Nat. Commun., vol. 5, pp. 1–7, 2014, doi: 10.1038/ncomms5449.

[17] C. Chen et al., "Highly Flexible and Efficient Solar Steam Generation Device," Adv. Mater., vol. 29, no. 30, pp. 1–8, 2017, doi: 10.1002/adma.201701756.

[18] Y. Li et al., "Graphene oxide-based evaporator with one-dimensional water transport enabling high-efficiency solar desalination," Nano Energy, vol. 41, pp. 201–209, 2017, doi: 10.1016/j.nanoen.2017.09.034.

[19] P. Patsalas, N. Kalfagiannis, and S. Kassavetis, "Optical properties and plasmonic performance of titanium nitride," Materials (Basel)., vol. 8, no. 6, pp. 3128–3154, 2015, doi: 10.3390/ma8063128.

[20] A. Reinholdt et al., "Structural, compositional, optical and colorimetric characterization of TiN-nanoparticles," Eur. Phys. J. D, vol. 31, no. 1, pp. 69–76, 2004, doi: 10.1140/epjd/e2004-00129-8.

[21] U. Guler, S. Suslov, A. V. Kildishev, A. Boltasseva, and V. M. Shalaev, "Colloidal Plasmonic Titanium Nitride Nanoparticles: Properties and Applications," Nanophotonics, vol. 4, no. 1, pp. 269–276, 2015, doi: 10.1515/nanoph-2015-0017.

[22] S. Ishii, R. P. Sugavaneshwar, and T. Nagao, "Titanium Nitride Nanoparticles as Plasmonic Solar Heat Transducers," J. Phys. Chem. C, vol. 120, no. 4, pp. 2343–2348, 2016, doi: 10.1021/acs.jpcc.5b09604.

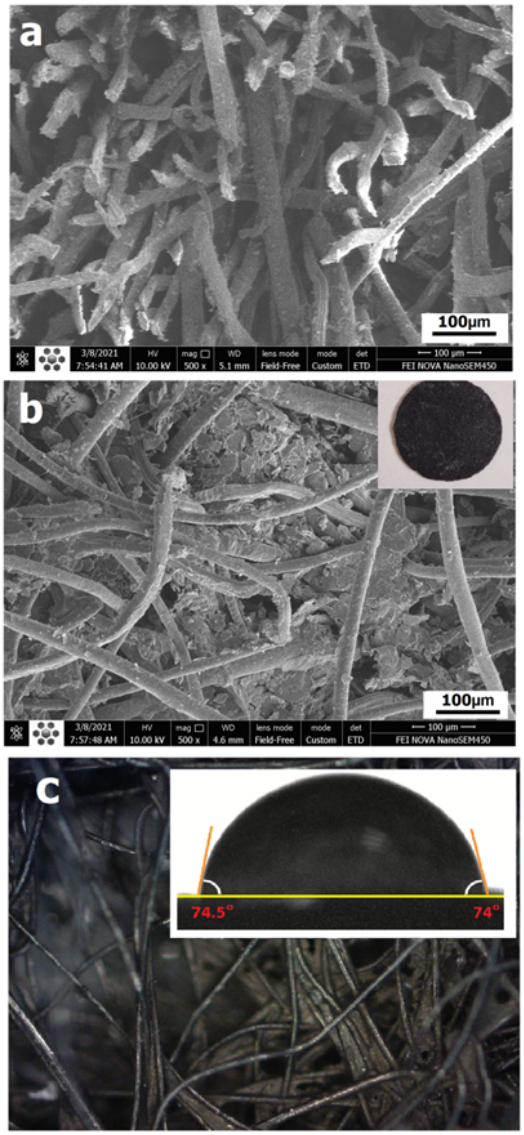

Fig. 3. (a) FESEM images of pure felt (b) FESEM images of absorber surface (TiN 0.27 wt%); (c) Optical microscopy images of the absorber surface.

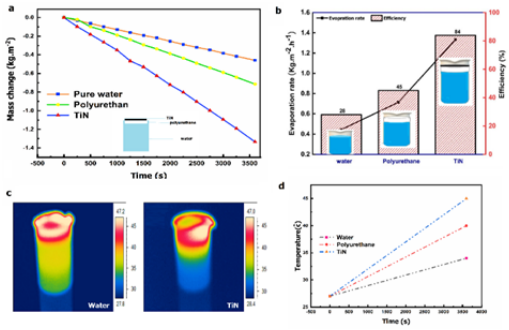

Fig. 4. (a) Solar water evaporation performance of TiN 0.27 wt% under one-sun, PU system, and uncovered water as the reference sample; (b) corresponding evaporation rates (black square) and solar-vapor conversion efficiency (red column) of the systems; (c) Thermal profile of the systems (uncovered water and TiN75); (d) Temperature change diagram.